SERBIAN JOURNAL OF ELECTRICAL ENGINEERING
Vol. 9, No. 2, June 2012, 189-200

UDK: 621.315.1.064.2 **DOI: 10.2298/SJEE1202189M**

Accurate Fault Location Algorithm on Power Transmission Lines with use of Two-end Unsynchronized Measurements

Dine Mohamed[1], Sayah Houari[1], Bouthiba Tahar[2]

Abstract: This paper presents a new approach to fault location on power transmission lines. This approach uses two-end unsynchronised measurements of the line and benefits from the advantages of digital technology and numerical relaying, which are available today and can easily be applied for off-line analysis. The approach is to modify the apparent impedance method using a very simple first-order formula. The new method is independent of fault resistance, source impedances and pre-fault currents. In addition, the data volume communicated between relays is sufficiently small enough to be transmitted easily using a digital protection channel. The proposed approach is tested via digital simulation using MATLAB and the applied test results corroborate the superior performance of the proposed approach.

Keywords: Fault location, Unsynchronized measurements, Communication, MATLAB.

1 Introduction

Rapid grow of power system grids during last years caused an increase in both the number of lines and their total length. Along with power energy consumption rise, a continuous and reliable energy supply is demanded. Transmission lines are essential parts of a power system for power energy delivery from generating plants to end customers. They are a part of the system where faults occur most likely. These faults result mostly from mechanical failures and have to be removed before re-energization of the line. Accurate fault location is highly required by operators and utility staff to expedite service restoration, reduce outage time, operating costs and customer complains. Fault location is still the subject of rapid further developments. Research efforts are focused on developing efficient fault location algorithms intended for application to more and more complex networks [1, 2].

[1]Université Djillali Liabes, Faculté de Génie Electrique B.p N° 89 Sidi Bel Abbes Algérie, ICEPS (Intelligent Control Electrical Power System) Laboratory; E-mail: dinemohamed83@yahoo.fr, housayah@yahoo.fr
[2]Université des Sciences et de la Technologie d'Oran Faculté de Génie Electrique B. P. 1505 EL Mnaouer, Oran, Algérie; E-mail: tbouthiba@yahoo.com

Varieties of fault location algorithms have been developed so far. The majority of them are based on an impedance principle, making use of the fundamental frequency voltages and currents. Depending on the availability of the fault locator input signals, they can be categorized as the following:

- one-end algorithms [2],
- two-end algorithms [5 – 9].

One-end impedance-based fault location algorithms estimate a distance to fault with the use of voltages and currents acquired at a particular end of the line. Such a technique [2] is simple and does not require communication means with the remote end. Therefore, it is attractive and is commonly incorporated into the microprocessor-based protective relays. However, it is subject to several sources of error, such as the reactance effect, the line shunt capacitance, and the fault resistance value [4, 5].

Two-end algorithms [5 – 9] process signals from both terminals of the line and thus larger amount of information [5 – 9] is utilized. Performance of the two-end algorithms is generally superior in comparison to the one-end approaches. Different input signals are used for two-end fault locators as, for example, complete currents and voltages from the line terminals [5 – 7] or quantities from impedance relays at the line terminals [8 – 9].

Digital measurements at different line terminals can be performed synchronously if the global positioning system (GPS) [3] is available. Otherwise, or in case of loss of the signal from the GPS, the digital measurements from the line terminals are acquired asynchronously and, thus, do not have a common time reference. Synchronized two-end measurements allow simple and accurate fault location [5, 10].

One class of two-terminal impedance-based methods makes use of unsynchronized data. The main advantage of such methods is the lower cost of implementation, since there is no need to use global positioning system (GPS) or other devices to provide a common time base for the measurement instruments of the two ends.

This paper delivers the fault location algorithm, which calculates a distance to fault by processing unsynchronized two-end measurements of voltages and currents with calculation of the synchronization angle. However, the delivered algorithm differs substantially from the earlier approaches [6, 7]. First, the unknown synchronization angle (6) is determined with the Newton-Raphson iterative procedure, After providing the synchronization of the measurements from two different ends of the line [5], the distance to fault calculation is performed directly.

2 Fault Location Approach

2.1 Principle

Fig. 1 presents schematically the considered two-end fault location on two-terminal transmission line AB. The fault locator (FL) is here shown as a stand-alone device, however, it can be also associated with the measurement unit at either side of the line (MUA or MUB).

The mesured voltage and currents are extracted, filtred with analogue fiters using the second order Butterworth model with cut-off frequency equal to 300Hz and sampled. Fault location was performed by estimating the phasors with the use of the DFT algorithm working with 20 samples per cycle.

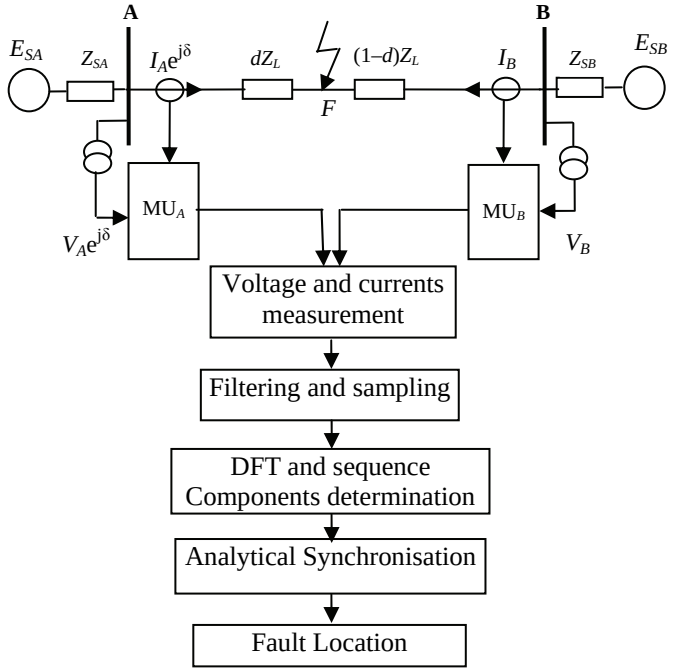

Fig. 1 – *Schematic diagram for two-end unsynchronized fault location.*

In case of two-end unsynchronized measurements [6 – 9] the sampling instants at the A and B ends (marked in Fig. 2 by small circles) do not coincide due to lack of the GPS control.

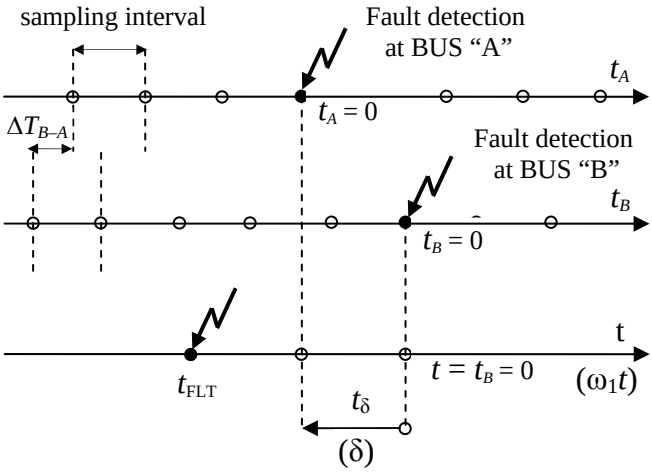

Fig. 2 – *Need for phase alignment in case of using two-end unsynchronized measurements.*

As a result of not using the GPS control, a certain random shift (ΔT_{B-A}) exists between the sampling instants of the both ends. Moreover, the instant at which the fault is detected is usually considered as the time stamp: $t_A = 0$ (at the bus A) and $t_B = 0$ (at the bus B), which also do not coincide. In consequence, the measurements from both ends do not have a common time base. In order to assure such common base one has to take the measurements from the particular end as the base (for example from the terminal B, as it will be assumed in all further considerations), while for the other terminal (the terminal A) needs to introduce the respective alignment. In case of formulating the fault location algorithm in terms of phasors of the measured quantities, phase alignment is done by multiplying all the phasors from the terminal A by the synchronization operator $e^{j\delta}$, where δ is synchronization angle.

2.2 Use of two-end voltages and current unsynchronized measurements

The distributed-parameter model of a faulted line for the *i*-th symmetrical component, with use of the correction factors for representing series and shunt parameters, as in Fig. 3, is taken into consideration. The voltage at fault point (F), viewed from the terminals A and B, respectively, is expressed as follows:

$$V_{Fi}^{A} = [V_{Ai}\cosh(\gamma_i l d) - Z_{ciL} I_{Ai}\sinh(\gamma_i l d)]e^{j\delta}, \quad (1)$$

$$V_{Fi}^{B} = V_{Bi}\cosh(\gamma_i l(1-d)) - Z_{ciL} I_{Bi}\sinh(\gamma_i l(1-d)), \quad (2)$$

where: V_{Ai}, I_{Ai}, V_{Bi} and I_{Bi} are phasors of the *i*-th symmetrical component of voltages and currents obtained from measurements at the line terminals.

$$e^{j\delta} = \cos(\delta) + j\sin(\delta), \tag{3}$$

δ : synchronization angle,

l: length of the line (km),

$\gamma_i = \sqrt{Z'_{iL} Y'_{iL}}$: propagation constant of the line for the i-th symmetrical component,

$Z_{ciL} = \sqrt{Z'_{iL} / Y'_{iL}}$: characteristic impedance of the line for the i-th symmetrical component,

$Z'_{iL} = R'_{iL} + j\omega L'_{iL}$: impedance of the line for the i-th symmetrical component (Ω /km),

$Y'_{iL} = G'_{iL} + j\omega C'_{iL}$: admittance of the line for the i-th symmetrical component (F/km),

R'_{iL}, L'_{iL}, G'_{iL}, C'_{iL} : resistance, inductance, conductance and capacitance of the line for the i-th symmetrical component.

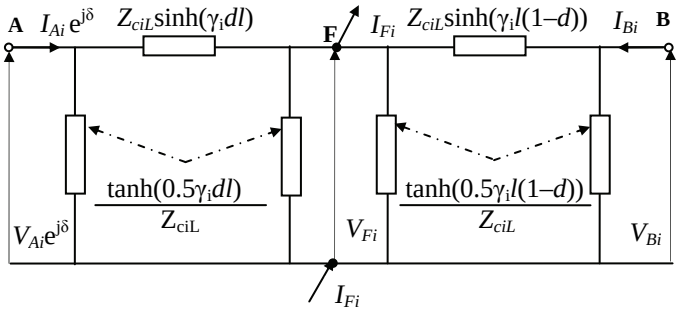

Fig. 3 – *Distributed-parameter model of faulted transmission line for the i-th symmetrical component.*

After taking into account the following trigonometric identities:

$$\cosh(\gamma_i l(1-d)) = \cosh(\gamma_i l)\cosh(\gamma_i ld) - \sinh(\gamma_i l)\sinh(\gamma_i ld), \tag{4}$$

$$\sinh(\gamma_i l(1-d)) = \sinh(\gamma_i l)\cosh(\gamma_i ld) - \cosh(\gamma_i l)\sinh(\gamma_i ld), \tag{5}$$

and performing further rearrangements, the formula (2) can be presented as:

$$V_{Fi}^{B} = F_i \cosh(\gamma_i ld) + H_i \sinh(\gamma_i ld), \tag{6}$$

where:

$$F_i = V_{Bi}\cosh(\gamma_i l) - Z_{ciL} I_{Bi} \sinh(\gamma_i l), \tag{7}$$

$$G_i = -V_{Bi}\sinh(\gamma_i l) + Z_{ciL} I_{Bi} \cosh(\gamma_i l). \tag{8}$$

The voltages (1) and (2), as present at the same fault point (F), are to be compared:

$$V_{Fi}^{A} = V_{Fi}^{B}. \tag{9}$$

Performing such a comparison results in obtaining :

$$X_i \sinh(\gamma_i l d) + N_i \cosh(\gamma_i l d) = 0, \tag{10}$$

where:

$$X_i = V_{Bi} \sinh(\gamma_i l) - Z_{ciL} I_{Bi} \cosh(\gamma_i l) - Z_{ciL} I_{\mathrm{A}i} e^{\mathrm{j}\delta}, \tag{11}$$

$$N_i = V_{Bi} \cosh(\gamma_i l) - Z_{ciL} I_{Bi} \cosh(\gamma_i l) - \mathrm{V}_{\mathrm{A}i} e^{\mathrm{j}\delta}, \tag{12}$$

From (10) one obtains the following formula for the distance to fault, with use of the *i*-th symmetrical component of voltages and currents obtained from measurements at the line terminals:

$$d = \frac{1}{\gamma_i l} \tanh^{-1}\left[\frac{V_{Bi} \cosh(\gamma_i l) - Z_{ciL} I_{Bi} \sinh(\gamma_i l) - \mathrm{V}_{\mathrm{A}i} e^{\mathrm{j}\delta}}{V_{Bi} \sinh(\gamma_i l) - Z_{ciL} I_{Bi} \cosh(\gamma_i l) - Z_{ciL} I_{\mathrm{A}i} e^{\mathrm{j}\delta}} \right]. \tag{13}$$

2.3 Determination of synchronization angle

Usage of the formula (13) requires prior determination of the synchronization operator ($e^{j\delta}$) since in the presented approach it does not go cancellation, as it was in [3, 4]. The unknown synchronization angle can be calculated with using the pre-fault [6] or fault quantities [7]. This paper proposes to determine the synchronization angle also from the fault quantities, however in the substantially different way.

The algorithm presented here applies elimination of the synchronization angle as a result of the applied mathematical manipulations. It starts with considering the lumped model of the faulted line while disregarding the shunt parameters (Fig. 4).

Comparison of the *i*-th symmetrical component of voltage at fault point (V_{Fi}), viewed from both A and B ends gives:

$$V_{Ai} \mathrm{e}^{\mathrm{j}\delta} - d Z_{iL} I_{\mathrm{A}i} \mathrm{e}^{\mathrm{j}\delta} = V_{Bi} - (1-d) \mathrm{Z}_{iL} \mathrm{I}_{Bi}. \tag{14}$$

Resolving (14) into real and imaginary parts gives:

$$\begin{aligned} &\mathrm{Re}(V_{Ai}) \sin\delta + \mathrm{Im}(V_{Ai}) \cos\delta - \mathrm{Im}(V_{Bi}) + C_{4i} = \\ &= d(C_{1i} \sin\delta + C_{2i} \cos\delta + C_{4i}), \end{aligned} \tag{15}$$

$$\begin{aligned} &\mathrm{Re}(V_{Ai}) \cos\delta - \mathrm{Im}(V_{Ai}) \sin\delta - \mathrm{Re}(V_{Bi}) + C_{3i} = \\ &= d(C_{1i} \cos\delta - C_{2i} \sin\delta + C_{3i}). \end{aligned} \tag{16}$$

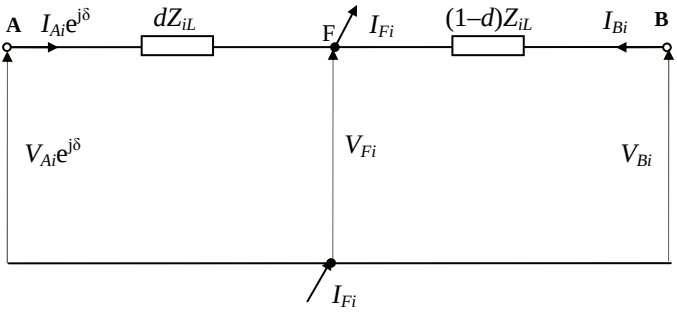

Fig. 4 – *Lumped model of faulted line for the i-th symmetrical component.*

The coefficients C_{1i}, C_{2i}, C_{3i}, and C_{4i}, in equations (15) and (16) are defined as:

$$C_{1i} = \mathrm{Re}(Z_{iL})\,\mathrm{Im}(\mathrm{I}_{Ai}) - \mathrm{Im}(Z_{iL})\,\mathrm{Re}(\mathrm{I}_{Ai}), \tag{17}$$

$$C_{2i} = \mathrm{Re}(Z_{iL})\,\mathrm{Im}(\mathrm{I}_{Ai}) + \mathrm{Im}(Z_{iL})\,\mathrm{Re}(\mathrm{I}_{Ai}), \tag{18}$$

$$C_{3i} = \mathrm{Re}(Z_{iL})\,\mathrm{Re}(\mathrm{I}_{Bi}) - \mathrm{Im}(Z_{iL})\,\mathrm{Im}(\mathrm{I}_{Bi}), \tag{19}$$

$$C_{4i} = \mathrm{Re}(Z_{iL})\,\mathrm{Im}(\mathrm{I}_{Bi}) + \mathrm{Im}(Z_{iL})\,\mathrm{Re}(\mathrm{I}_{Bi}). \tag{20}$$

The next step is to divide (15) by (16) to form one equation with one unknown δ. After rearranging this equation and cancelling a number of terms, the resulting equation is:

$$\mathrm{A}_1\cos(\delta)+\mathrm{A}_2\sin(\delta) + \mathrm{A}_3 = 0 \tag{21}$$

$$\begin{aligned}\mathrm{A}_{1i} = &-C_{3i}\,\mathrm{Re}(\mathrm{V}_{Ai}) - C_{4i}\,\mathrm{Im}(\mathrm{V}_{Ai}) - C_{1i}\,\mathrm{Re}(\mathrm{V}_{Bi}) - \\ &-C_{2i}\,\mathrm{Im}(\mathrm{V}_{Bi}) + C_{1i}C_{3i} + C_{2i}C_{4i},\end{aligned} \tag{22}$$

$$\begin{aligned}\mathrm{A}_{2i} = &\,C_{4i}\,\mathrm{Re}(\mathrm{V}_{Ai}) - C_{3i}\,\mathrm{Im}(\mathrm{V}_{Ai}) - C_{2i}\,\mathrm{Re}(\mathrm{V}_{Bi}) + \\ &+C_{1i}\,\mathrm{Im}(\mathrm{V}_{Bi}) + C_{2i}C_{3i} - C_{1i}C_{4i},\end{aligned} \tag{23}$$

$$\mathrm{A}_{3i} = C_{2i}\,\mathrm{Re}(\mathrm{V}_{Ai}) - C_{1i}\,\mathrm{Im}(\mathrm{V}_{Ai}) - C_{4i}\,\mathrm{Re}(\mathrm{V}_{Bi}) + C_{3i}\,\mathrm{Im}(\mathrm{V}_{Bi}). \tag{24}$$

The equation for the synchronization angle can be solved using the method outlined below.

2.3.1 Newton Raphson solution

Equation (21) has one unknown δ (the synchronization angle) and can be solved by an iterative Newton-Raphson method. The equations for the iterative calculation of the angle δ (radian) are:

$$\delta_{k+1} = \delta_k + \frac{F(\delta_k)}{F'(\delta_k)}, \tag{25}$$

$$F(\delta_k) = A_{2i}\cos\delta_k + A_{1i}\sin\delta_k + A_{3i}, \tag{26}$$

$$F'(\delta_k) = A_{1i}\cos\delta_k - A_{2i}\sin\delta_k. \tag{27}$$

The iterative procedure is stopped when the difference between the last two calculations is smaller than a preassigned limit (e.g., $\delta_{k+1} - \delta_k \leq 10^{-4}$). This method has a quadratic convergence and an initial guess is required, but this Is not considered a practical problem. If the angles of the voltages from both ends are set to zero, the angle δ becomes the apparent angle between the voltages and does not depend on the synchronization error, In practice, this angle i s in a limited range around zero. Thus, by setting the initial angle to zero, the algorithm has been observed to converge rapidly in numerous tests. Once the synchronization angle is known, the fault location can be calculated either from equation (13).

3 Evaluation

MATLAB simulation program was applied to evaluate performance of the developed fault location algorithm. Different two-terminal networks were modeled for generation of fault data used in evaluation of the presented fault location algorithm. In particular, 345 kV power network containing the two-terminal line with the sections: l = 100 km (**Table 1**).

Table 1
Parameters of the 345 kV *transmission line.*

Component:	Parameter:	
Line AB	l	100 km
	Z'_{1L}	(0.0275 + j0.422) Ω/km
	Z'_{0L}	(0.275 + j1.169) Ω/km
	C'_{1L}	9.483 nF/km
	C'_{0L}	6.711 nF/km
Equivalent system at terminal A	Z_{1SA}	(0.238 + j6.19) Ω
	Z_{0SA}	(0.833 + j5.12) Ω
	Angle of EMF from phase ‘a’	0°
Equivalent system at terminal B	Z_{1SB}	(0.238 + j5.72) Ω
	Z_{0SB}	(2.738 + j10) Ω
	Angle of EMF from phase ‘a’	15^0

All signals obtained from MATLAB simulations are naturally perfectly synchronized. In order to test the delivered algorithm the intentional unsynchronization has been introduced, namely: all signals from the bus A

delayed by 18°, i.e. the real value of the synchronization angle: $\delta_{real} = 18^o$ (note: this delay corresponds to the single sampling interval for 50 Hz signals digitalized at 1000 Hz). The continuous values results were singled by averaging within the interval (50, 70) ms after the fault inception.

Fig. 4 shows the waveforms of the input signals. For this far end fault (d = 10 km) and fault resistance ($R_F = 5\Omega$).

In Fig. 5 to Fig. 8, the example of fault location is presented. The specifications of the fault – a-g fault, distance to fault: (d = 50 km for Fig. 7, d = 90 km for Fig. 8, fault resistance: $R_F = 5\Omega$, actual synchronization angle: $\delta_{real} = 18^o$ (obtained by introducing a delay of signals from the side A by 1 sample).

Table 2

Determination of the synchronization angle with use of positive sequence quantities (*a-g fault*, $R_F = 5\ \Omega$, $\delta_{real} = 18^o$).

	Calculated synchronization angle: δ (°) in particular 'iterations'		
dr(km)	'1'	'2'	'3'
10	19.68	18.02	18.01
20	20.05	18.08	18.06
30	20.50	18.13	18.11
40	20.84	18.18	18.14
50	21.03	18.21	18.21
60	21.05	18.24	18.21
70	20.89	18.26	18.23
80	20.56	18.27	18.26
90	20.02	18.25	18.24

Table 3

Determination of the distance to fault with use of positive sequence quantities (*a-g fault*).

$R_f = 0\ \Omega$			$R_f = 5\ \Omega$		$R_f = 10\ \Omega$	
dr (km)	*dc* (km)	e (%)	*dc* (km)	e (%)	*dc* (km)	e (%)
10	9.96	0.04	10.15	0.15	9.58	0.42
20	19.84	0.16	19.65	0.35	19.45	0.55
30	29.82	0.18	29.60	0.40	29.39	0.61
40	39.85	0.15	39.61	0.39	39.39	0.61
50	49.91	0.09	49.66	0.34	49.42	0.58
60	59.98	0.02	59.71	0.29	59.46	0.54
70	70.02	0.02	69.74	0.26	69.48	0.52
80	80.02	0.02	79.72	0.28	79.47	0.53
90	89.93	0.07	89.62	0.38	89.42	0.52

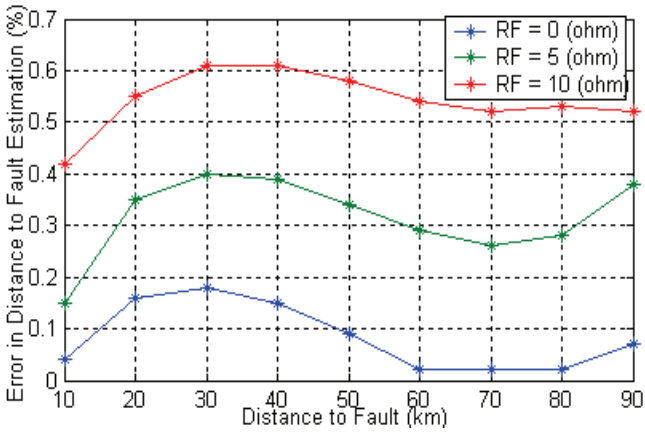

Fig. 5 – *Fault location* error[%] *for different fault resistance.*

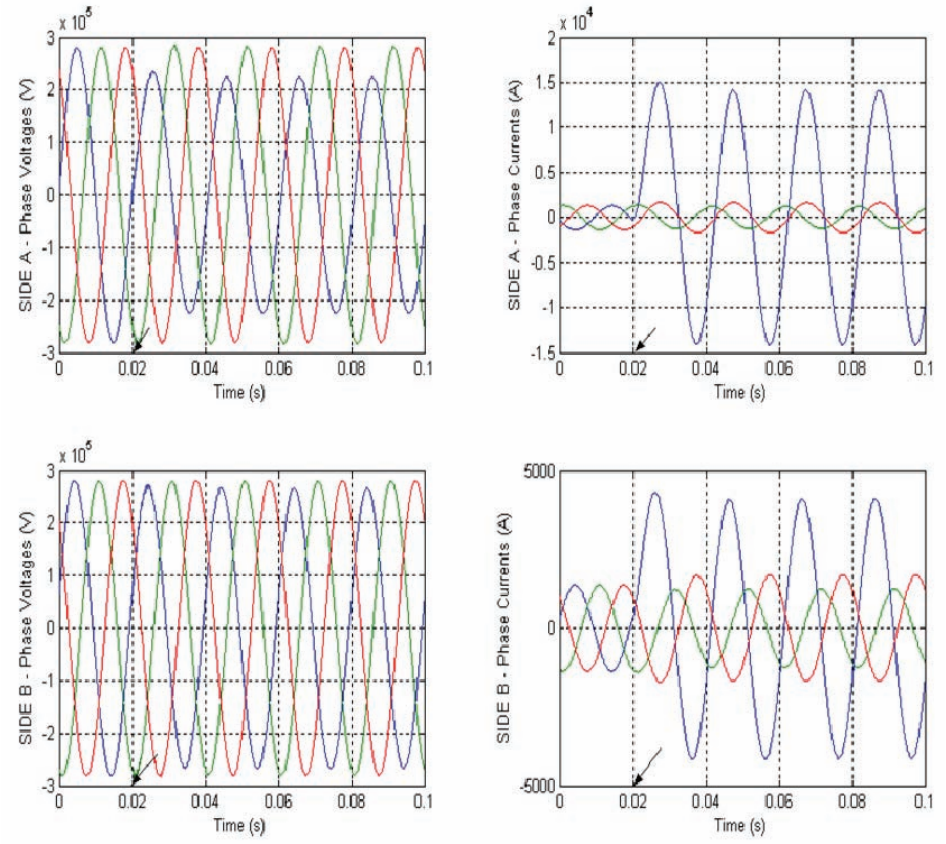

Fig. 6 – *The example – input signals of the fault location algorithm.*

Testing showed accuracy of fault location to be satisfactory. Maximum fault location error only slightly exceeds 0.6%.

Different specifications of faults have been considered in the evaluation analysis. The results of this analysis are presented in **Tables 2** and **3**.

In **Table 2** the results of the synchronization angle for the a-g faults, applied through fault resistance, $R_F = 5\ \Omega$ at different locations: d = 10–90 km with use of Newton–Raphson calculations. This method improvise very fast convergence, it is sufficient to perform only a third iteration of the calculations. In turn, **Table 3** present the results for the a-g faults involving the fault resistances $R_F = 0$–$10\ \Omega$.

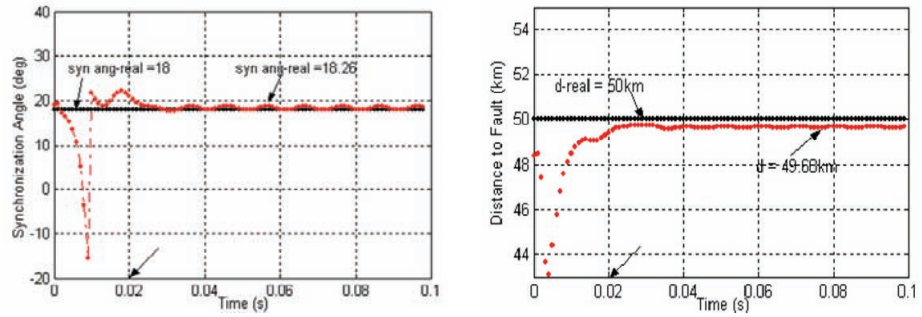

Fig. 7 – *The example* 1 – *a-g fault* (*dreal* = 50 km, $R_F = 5\ \Omega$, $\delta_{real} = 18^{\circ}$).

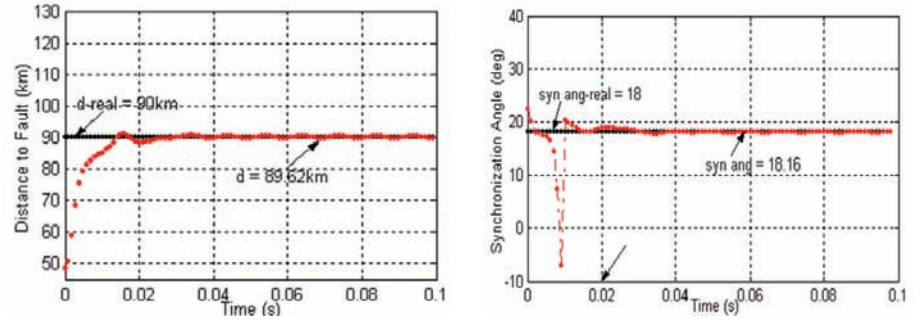

Fig. 8 – *The example* 2 – *a-g fault* (*dreal* = 90 km, $R_F = 5\ \Omega$, $\delta_{real} = 18^{o}$).

4 Conclusion

In this paper, the new accurate algorithm for locating faults on power transmission line with use of the two-end unsynchronized measurements of voltages and currents has been presented. Since numerical relays often store oscillographic and phasor information following the occurrence of a fault, the algorithm can be implemented using information which should be readily available. The substation computer and/or digital relay can process the data and estimate fault location with minimal assumptions, reducing the estimation error.

The test results have shown the benefits of two-terminal fault estimation when a fault resistance is present.

In summary, the algorithm highlights include :

- Synchronization of data is not required.
- Fault resistance and infeed do not influence fault location calculation.
- Fault type selection and pre-fault data are not required.
- Accurate compensation for long lines is available.
- Even with synchronized phasors, this algorithm should be used to compensate for phase delay or different sampling rates of the different recording devices.

The two-terminal approach also has additional advantages in that post-fault analysis is more accurate than before. By knowing the fault type and location more accurately, utilities should be able to reduce outage time and improve the quality of power delivery.

5 References

[1] L. Eriksson, M.M. Saha, G.D. Rockefeller: An Accurate Fault Locator with Compensation for Apparent Reactance in the Fault Resistance Resulting from Remote-end Infeed, IEEE Transaction on Power Apparatus and Systems, Vol. PAS-104, No. 2, Feb. 1985, pp. 423 – 436.

[2] T. Kawady, J. Stenzel: A Practical Fault Location Approach for Double Circuit Transmission Lines using Single End Data, IEEE Transaction on Power Delivery, Vol. 18, No. 4, Oct. 2003, pp. 1166 – 1173.

[3] P.A. Crossley, E. Southern: The Impact of the Global Positioning System (GPS) on Protection and Control, 11th International Conference on Power System Protection, Bled, Slovenia, 30 Sept. – 2 Oct. 1998, pp. 1 – 5.

[4] R.K. Aggarwal, D.V. Coury, A.T. Johns, A. Kalam: A Practical Approach to Accurate Fault Location on Extra High Voltage Teed Feeders, IEEE Transaction on Power Delivery, Vol. 8, No. 3, July 1993, pp. 874 – 883.

[5] M. Kezunovic, B. Perunicic: Automated Transmission Line Fault Analysis using Synchronized Sampling at Two Ends, IEEE Transaction on Power Systems, Vol. 11, No. 1, Feb. 1996, pp. 441 – 447.

[6] D. Novosel, D.G. Hart, E. Udren, J. Garitty: Unsynchronized Two-terminal Fault Location Estimation, IEEE Transaction on Power Delivery, Vol. 11, No. 1, Jan. 1996, pp. 130 – 138.

[7] M.S. Sachdev, R. Agarwal: A Technique for Estimating Transmission Line Fault Locations from Digital Distance Relay Measurements, IEEE Transaction on Power Delivery, Vol. 3, No. 1, Jan. 1988, pp. 121 – 129.

[8] J. Izykowski, R. Molag, E. Rosolowski, M.M. Saha: Accurate Location of Faults on Power Transmission Lines with use of Two-end Unsynchronized Measurements, IEEE Transaction on Power Delivery, Vol. 21, No. 2, April 2006, pp. 627 – 633.

[9] I. Zamora, J.F. Minambres, A.J. Mazon, R. Alvarez-Isasi, J. Lazaro: Fault Location on Two-terminal Transmission Lines based on Voltages, IEE Proceedings – Generation, Transmission and Distribution, Vol. 143, No. 1, Jan. 1996, pp. 1 – 6.

[10] M.M. Saha, J. Izykowski, E. Rosolowski, R. Molag: ATP EMTP Investigation of a New Algorithm for Locating Faults on Power Transmission Lines with use of Two-end Unsynchronized Measurements, International Conference on Power Systems Transients, Lyon, France, 4 – 7 June.